

Physical and chemical characterisation of crude meat and bone meal combustion residue: “waste or raw material?”

Eric Deydier^{a,*}, Richard Guilet^a, Stéphanie Sarda^a, Patrick Sharrock^b

^a *Laboratoire de Chimie Inorganique et Santé, Université Paul Sabatier, IUT A, Avenue Georges Pompidou, 81100 Castres, France*

^b *LCBM, Université Paul Sabatier, Avenue Georges Pompidou, 81100 Castres, France*

Received 28 October 2004; received in revised form 1 February 2005; accepted 1 February 2005

Available online 9 March 2005

Abstract

As a result of the recent bovine spongiform encephalopathy (BSE) crisis in the European beef industry, the use of animal by-product is now severely controlled. Meat and bone meal (MBM) production can no longer be used to feed cattle and must be safely disposed of or transformed. Main disposal option is incineration, producing huge amounts of ashes the valorisation of which becomes a major concern. The aim of this work is to characterise MBM combustion residue in order to evaluate their physical and chemical properties to propose new valorisation avenues. The thermal behaviour of crude meat and bone meal was followed by thermogravimetric analysis (TGA) and (24 wt.%) inorganic residue was collected. The resulting ashes were characterised by powder X-ray diffraction (XRD), particle size distribution, specific surface area (BET), scanning electron microscopy (SEM) couple with energy disperse X-ray analysis (EDX). Elemental analysis revealed the presence of chloride, sodium, potassium, magnesium with high level of phosphate (56 wt.%) and calcium (31 wt.%), two major constituents of bone, mainly as a mixture of $\text{Ca}_{10}(\text{PO}_4)_6(\text{OH})_2$ and $\text{Ca}_3(\text{PO}_4)_2$ phases. The impact of combustion temperature (from 550 to 1000 °C) on the constitution of ashes was followed by TGA, XRD and specific surface measurements. We observed a strong decrease of surface area for the ashes with crystallisation of calcium phosphates phases without major changes of chemical composition.

© 2005 Elsevier B.V. All rights reserved.

Keywords: Meat and bone meal; Apatite; Ashes; Phosphate sources; Valorisation

1. Introduction

As a result of the recent bovine spongiform encephalopathy (BSE) crisis in the European beef industry, the use of animal by-products is now severely restricted. Indeed, the transmissible spongiform encephalopathy agent (SPE agent), also named scrappy prion, is responsible for fatal neurodegenerative diseases in animals and humans [1–4]. Nowadays, brain, spinal cord, tonsils, etc. and sick animal corpses are considered as high risk wastes and must be incinerated. Safe animal wastes (meat and bones) coming from slaughterhouse waste are mixed, crushed and cooked together. After the cooking process, tallow is extracted and the remaining residue, known as meat and bone meal (MBM) or animal flour, is sterilised

before being safely disposed off [5–7]. This sterilised product is called low risk MBM. Since November 2000, low risk MBM can no longer be used to feed cattle but can be incorporated in food for pig, poultry, fish or animal pets. Their import to European Community (EU) and their export from EU is banned. Nowadays, the over production of low risk MBM must be eliminated or safely recycled [5–10].

Among the different processes studied, valorisation of MBM can be realised by a thermal degradation treatment (incineration or pyrolysis) [8–10], as they are readily flammable fuel (approximately $17,000 \text{ kJ kg}^{-1}$) [9]. During high temperature combustion (over 800 °C), thermal energy is recovered and proteins such as prions are destroyed (as all organic matter is converted to CO_2 , H_2O , etc.) [1–3]. Co-incineration in cement kilns is the most common way, for MBM destruction, used in France. They are mixed with cement compounds (calcium, silica, alumina, etc.) and heated over 1500 °C to pro-

* Corresponding author. Tel.: +33 5 63 62 11 54; fax: +33 5 63 35 63 88.
E-mail address: eric.deydier@iut-tlse3.fr (E. Deydier).

duce the clinker. In England, the use of MBM dedicated incinerator is developed. Incineration plants are set up in Glanford, Wyminton and Widnes with a joint capacity of 205,000 tons of MBM/year (ton = Mg).

In France, for example, 850,000 tons of MBM are produced each year but actually only 45% can be burned by cement plants [6]. The remaining 55% are stored waiting for further destruction or valorisation. Ashes produced by meat and bone meal combustion represent up to 30% of the original weight. Thermal treatment of the entire MBM production would lead to an important amount of ashes (nearly 250,000 tons/year). Therefore, the fate of meat and bone meal combustion residue stocks is of major environmental concern. Large storage costs for wastes classified as dangerous are also an economic burden.

As MBM combustion residues mainly arise from bone combustion, they contain a high amount of phosphate and calcium, two major constituents of bone. In our search for new valorisation ways we focus on phosphoric acid production, phosphate source for industry, agricultural soil enrichment, heavy metals immobilisation in soil or water, etc. as developed for other phosphate rich materials (rocks, hydroxypapatites, bone char, etc.) [11–30]. We report here a study on the physical and chemical characterisation of meat and bone meal combustion residues. The thermal behaviour of crude MBM was followed by thermogravimetric analysis (TGA). The impact of combustion temperature on the structure of ashes was followed by powder X-ray diffraction. The resulting ashes were characterised by elemental analysis, powder X-ray diffraction (XRD), particle size distribution, specific surface area (BET), scanning electron microscopy (SEM) and energy disperse X-ray analysis (EDX).

2. Materials and methods

Low risk sterilised meat and bone meal were provided by Fersobio. MBM were burned twice by calcination in an electric furnace programmed to reach 550 °C at 2°/min. During combustion, MBM particles melted and stucked together. The first combustion gave a black residue (carbon rich). This residue was mixed manually before a second combustion in order to complete decomposition and obtain clear ashes.

Thermogravimetric analysis was performed with a Setaram TG-DTA92 analyser, in a platinum crucible, under air or argon atmosphere, from 20 to 1000 °C with an increasing temperature rate of 3 °C/min. The mass of the samples used was 40 mg approximately.

Total C, H and N were determined by elemental analysis on a Thermoquest CHN EA 1108W. Specific surface area measurements were realised by applying a 5-points BET method (nitrogen adsorption at 77 K) on a Micromeritics Gemini Vacprep 061. Samples were previously degassed under vacuum at 100 °C.

Electron scanning microscopy (SEM) observations coupled with EDX analysis were performed on a Philips

ESEM XL30 environmental microscope. Infrared spectra were recorded with an ATI Mattson (Genesis series FTIR) spectrometer.

Powdered solids were analysed by X-ray diffractometry using a Siemens D501 diffractometer operating with Co K α radiation (1.78892 nm; 30 kV; 35 mA). Measurements were made using a step-scanning technique with 2θ step intervals of 0.029° from $0.29^\circ < 2\theta < 105^\circ$ and an acquisition time of 1 s/step. Phases were identified by comparing the pattern with JCPDS files (Joint Committee for powder diffraction standards).

Particle size analysis was performed on a laser (He–Ne at 632.8 nm) diffraction analyser (Mastersizer S, Malvern) equipped with a solution dispersion accessory (Hydro QSMU, Malvern) in pure ethanol solution. $D(V,0.5)$ and $D(V,0.9)$ values are the maximum particles size for particles representing, respectively 50 and 90% of sample volume.

Elements analysis was performed by atomic adsorption (AA) with flame atomisation (Unicam, solar, air/C₂H₂ gas mixture), with graphite furnace atomisation (Perkin-Elmer SIMA 6000) or inductively coupled plasma (ICP). Certified aqueous standards and matrix modifier [LaCl₃, Mg(NO₃)₂ and NH₄(H₂PO₄)] were obtained from Aldrich.

3. Results and discussion

3.1. MBM combustion

In our experiments we used low fat MBM coming from slaughterhouse waste. These products are dehydrated (110 °C/4–5 h) and sterilised (133 °C/20 min/3 bar) according to European standards by Fersobio. Resulting low risk MBM still contains water (3–8 wt.%) and large amount of fats (10–14 wt.%) and other organic compounds (25–35 wt.%) according to low risk MBM producers [6].

Thermal analysis of MBM is realised under air (combustion) and argon (pyrolysis) atmosphere with 3 °C/min temperature increase rate (Fig. 1). Combustion shows a three step mass loss with nearly 24% inorganic residue available. We can notice that the first two steps are similar in both experiments (air and Ar). The first step, in the temperature range of 50–150 °C, is attributed to water (6%) evaporation. The second step, observed between 180 and 300 °C, is due to evaporation of low molecular weight compounds and/or decompositions reactions. At last, the third weight loss between 250 and 500 °C, faster under air than under argon atmosphere, is a combustion stage, where all organic matter is decomposed to H₂O, CO₂, etc. Under our conditions, thermal decomposition is practically complete at 550 °C. Crude ashes represent 24 wt.% of the initial MBM. Elemental analysis reveals small amounts of carbon (0.97%), hydrogen (0.27%) and nitrogen (0.23%) confirming the inorganic nature of ashes. We notice that over 550 °C mass loss is stabilised, suggesting that the composition of the ashes remains almost unchanged. These results are in agreement with previous studies on

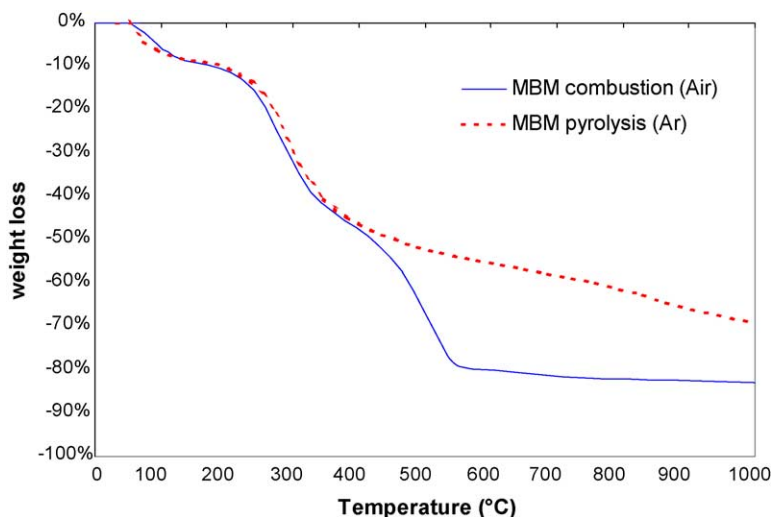


Fig. 1. Thermal behaviour of MBM under argon and air atmosphere.

thermal decomposition (combustion and pyrolysis) of MBM [8–10].

3.2. Ashes particle size distribution

Particle size distribution of ashes is relatively broad, from a few micrometre to a few millimetre, with irregular shape. After sieving, we observe that 11% (wt.%) of ash particles are bigger than 1 mm, 32% between 250 μm and 1 mm, and the remaining 57% smaller than 250 μm . Laser diffraction analysis of particles smaller than 250 μm shows that they are very heterogeneous, with $D(V,0.5)=50\ \mu\text{m}$ and $D(V,0.9)=245\ \mu\text{m}$. The large particle size distribution of ashes smaller than 250 μm is confirmed by scanning electron microscopy (SEM) where two groups of particles are clearly visible (Fig. 2).

However, according to a valorisation point of view (phosphoric acid production, phosphate source for industry, agricultural soil amendment, heavy metals immobilisation, etc.), ashes can be considered as homogenous material. Moreover, if necessary, larger particles can be easily grinded (by a centrifugal mill of agate balls for example), to reduce particle size dispersion.

3.3. Ashes chemical characterisation

EDX analysis of ashes, coupled to SEM, shows that all particles present similar composition with high levels of calcium, phosphorus, oxygen, sodium and much lower proportions of potassium, magnesium, chloride, sulfur and silicon. These last elements (Na, K, Mg, Cl, S, Si) are relatively more abundant in ash particles smaller than 250 μm , where iron traces are also encountered (Fig. 2). The strong C signal originates from the polymer adhesive sample support. Exact composition is realised after digestion of ashes in pure nitric acid (2 h reflux) and filtration to eliminate an insoluble residue representing nearly 5% of crude ashes (less than

1% of MBM). Concentrations of various elements in filtrate, determined by AA and ICP, are reported in Table 1. Calcium (nearly 31 wt.%) and phosphorus (around 18 wt.%) are major constituents, representing together 87 wt.% of ashes if

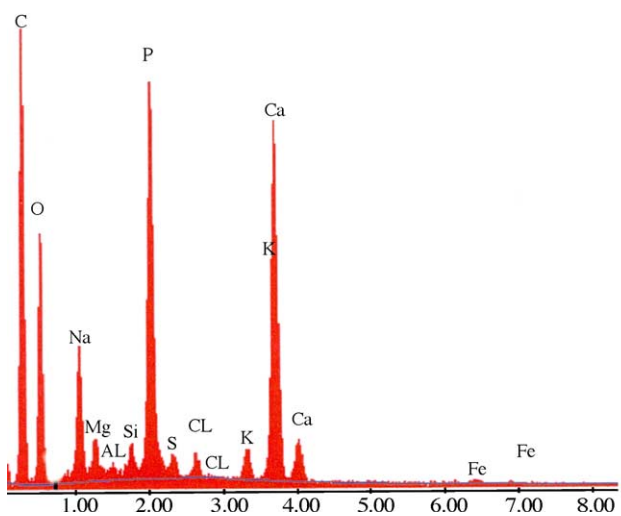
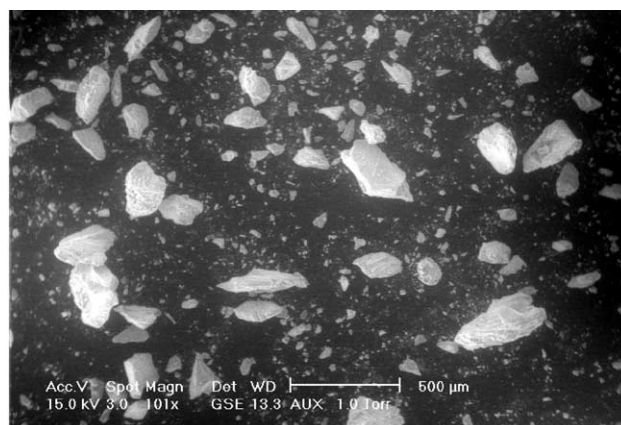


Fig. 2. Scanning electron microscopy and EDX analysis of crude MBM ashes (particles smaller than 250 μm).

Table 1
MBM combustion residue composition

	Ashes composition		Crude ashes
	<250 μm	>250 μm	
Main compounds content (wt.%)			
Water ^a	0.23	0.34	0.28
Phosphates ^b	55.29	57.71	56.33
Main elements content (>1 wt.%)			
Ca ^{c,d}	28.11	34.32	30.70
P ^c	18.03	18.85	18.37
Na ^c	3.53	1.572	2.68
K ^c	3.29	1.43	2.48
S ^c	1.78	1.26	1.55
Traces elements content (<1 wt.%)			
Mg ^c	0.95	0.59	0.79
Fe ^c	0.69	0.17	0.46
Zn ^c	0.08	0.03	0.06
Cu ^c	0.02	0.01	0.02
Al ^c	0.21	0.08	0.16
Si ^c	0.02	0.00	0.01

Non observed elements^c: Ba, Hg, Mn, Ni, Cr, Co, Cd, Ti, Ag, V, Li

^a ATG measurement.

^b Calculated value (considering all phosphorus are coming from phosphates).

^c ICP measurement.

^d AA measurement.

all phosphorus is converted to phosphates (56%). Sodium, potassium, magnesium and chloride represent nearly 10%.

At this point, it is interesting to compare these analytical results to natural phosphates rock analysis (14 samples) studied by Ma et al. [12]. We can first observe that calcium contain in ashes, nearly 31%, is in the average of measured values observed in rocks (27–35%). Phosphorus contain in ashes, nearly 18%, is slightly higher than in rocks (12–17%). We can also notice that ashes not only present higher level of phosphate, but they are also a purer phosphate source as nickel, chromium or cadmium have not been detected, whereas rocks contain up to a few hundreds ppm. These results allow us to reasonably expect that ashes could be a substitute for phosphate rich compounds.

Structural analysis was realised by IR and XRD. In IR, mainly strong split phosphate (PO_4^{3-}) bands are observed in the range $1100\text{--}1000\text{ cm}^{-1}$ (stretching mode) and $500\text{--}600\text{ cm}^{-1}$. These bands are characteristics of mineral phases of calcified tissues like bone or teeth, calcium hydroxyapatite, $\text{Ca}_{10}(\text{PO}_4)_6(\text{OH})_2$, being their major inorganic constituent [28,31]. Moreover, a small band at 875 cm^{-1} attributed to (HPO_4^{2-}) indicates the presence of calcium deficient apatite: $\text{Ca}_{10-x}(\text{HPO}_4)_x(\text{PO}_4)_{6-x}(\text{OH})_{2-x}$. These results can be correlated to high phosphorus and oxygen proportions in ashes measured by EDX. Broad carbonates bands

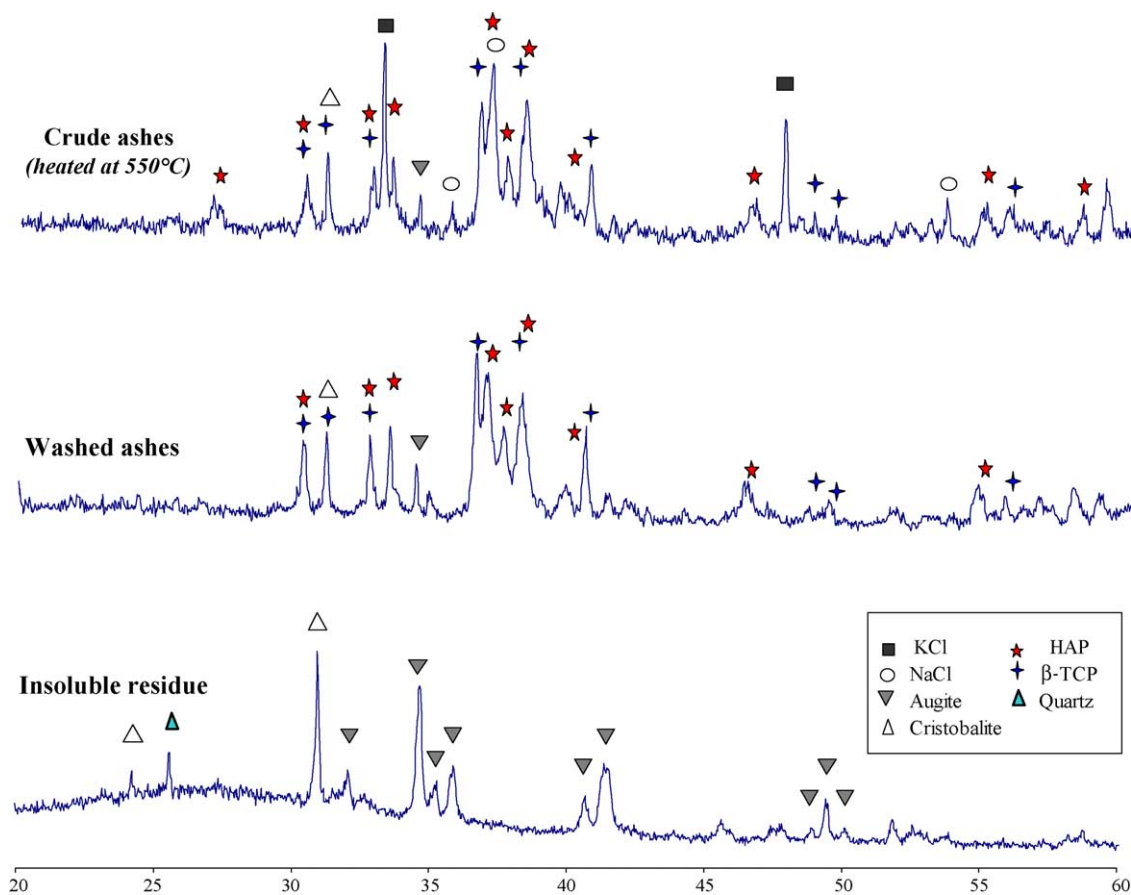


Fig. 3. XRD pattern of crude MBM ashes (particles smaller than $250\text{ }\mu\text{m}$), washed ashes and insoluble residue.

(1417 and 1457 cm^{-1}) are also observed, but with a much lower relative intensity compared to phosphates. We can also notice, that ash particles bigger than 250 μm present a higher level of carbonate than smaller particles (<250 μm).

The XRD pattern of crude ash particles smaller than 250 μm (Fig. 3) shows the presence of numerous phases. Previous results (composition and IR structural analysis) and comparison with JCPDS files allow us to propose an identification of this complex pattern. Calcium hydroxyapatite (CaHAP), tricalcium phosphate (β -TCP), sodium chloride (NaCl) and potassium chloride (KCl) have been clearly identified. Very water soluble NaCl and KCl, compared to CaHAP or β -TCP, can be easily extracted, as shown on the XRD pattern of the resulting washed ashes.

Peaks indicated with triangles on previous XRD spectra (Fig. 3), were also encountered in the insoluble residue produced during the mineralisation of ashes. EDAX analysis of this white insoluble powder shows a high level of silicon and oxygen with traces of sodium, calcium and magnesium (Fig. 4). On the other hand, IR analysis shows strong SiO bands in the range 1000–1200 cm^{-1} and at 460 cm^{-1} . The XRD pattern indicates the presence of both amorphous and crystallised phases. The numerous peaks obtained clearly suggest the presence of different phases. Comparison to JCPDS files leads us to propose the presence of cristoballite (SiO_2), quartz and augite (calcium sodium magnesium silicate mineral containing others metals such as Al). The presence of such minerals could be explained by cow alimentation, as particles of soil are swallowed by ruminants when they browse grass.

At last, particles bigger than 250 μm exhibit broad peaks similar to poor crystallised CaHAP phase with a significant amount of calcium carbonate (CaCO_3). This is in agreement with elemental analysis as we observe a carbon level three times higher (1.6%) than in particles smaller than 250 μm .

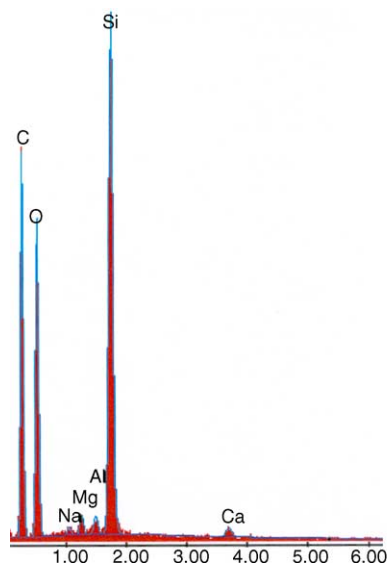


Fig. 4. Scanning electron microscopy and EDX analysis of the insoluble residue.

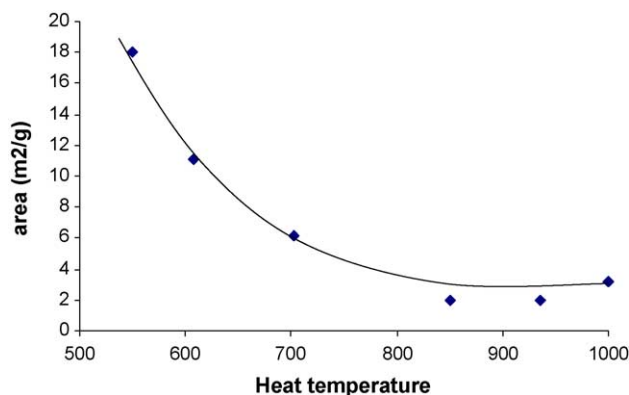


Fig. 5. Evolution of the surface area of ashes (smaller than 250 μm) vs. combustion temperature.

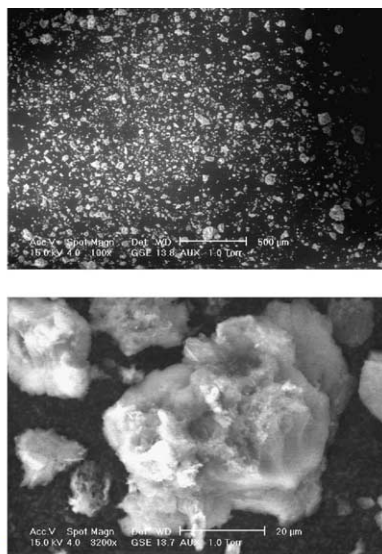
3.4. Thermal treatment of ashes

As ashes are produced by incineration, we also investigate the effect of thermal conditions on their structure. To allow an acute analysis, we focus our attention on particles smaller than 250 μm as their XRD pattern presents sharper peaks.

Ashes are submitted to higher temperatures, between 550 and 1000 $^{\circ}\text{C}$ with 2 $^{\circ}\text{C}/\text{min}$ heating rate. Elemental analysis of the different samples shows that the initial low levels of carbon (0.46 wt.%), hydrogen (0.43 wt.%) and nitrogen (0.27 wt.%) slightly decrease to less than 0.3% for carbon and hydrogen, values close to detection limits.

Surface area measurements of heat-treated ashes, from 550 to 1000 $^{\circ}\text{C}$ in air, show a dramatic decrease as temperature rises (Fig. 5). This is attributed to sintering of the particles. Similar results have been observed on heat-treated human and fish bones [32,33].

The XRD patterns of the different samples (Fig. 6) show that calcium phosphate peaks become sharper, when tempera-



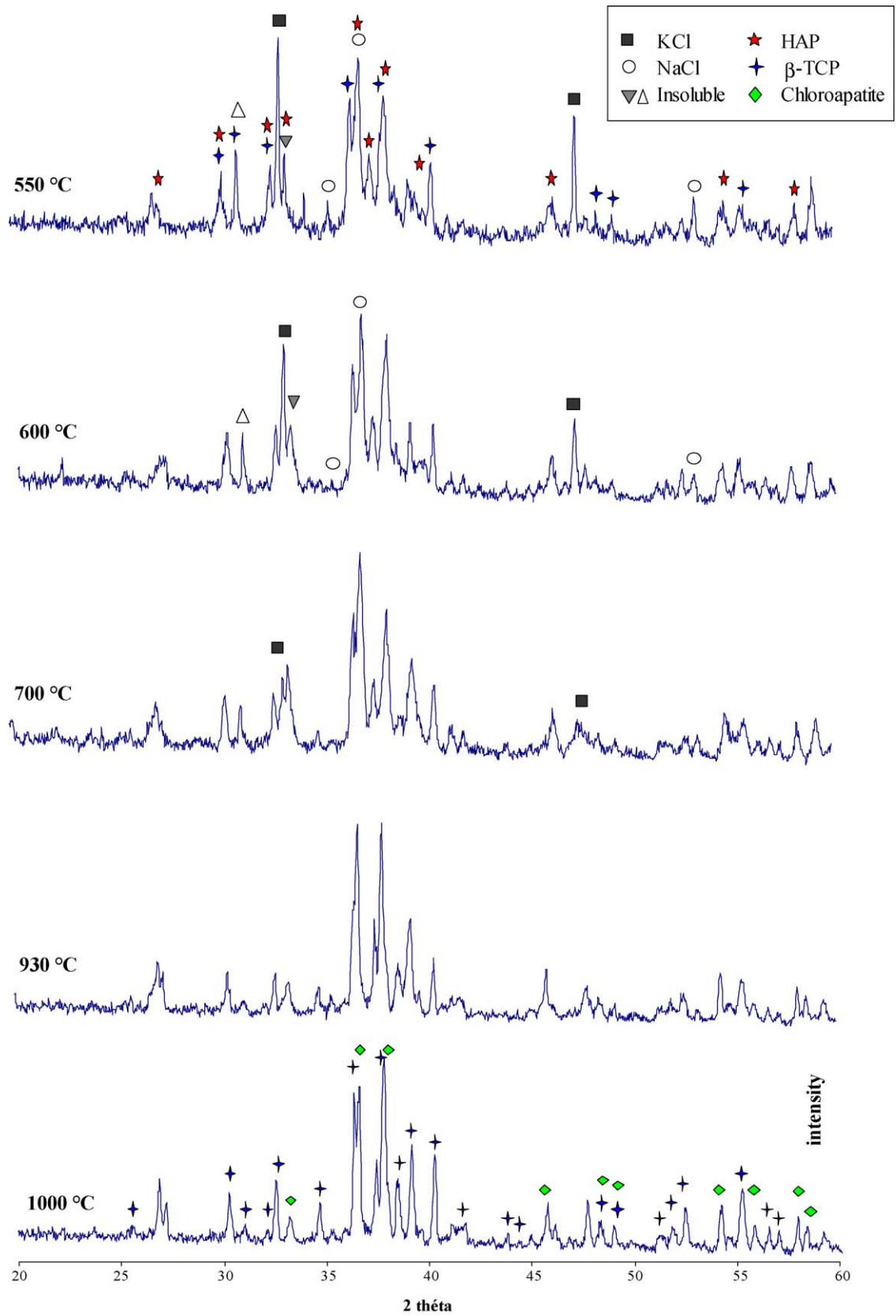


Fig. 6. Evolution of the XRD pattern of ashes (particles smaller than 250 μm) vs. combustion temperature.

ture rises, because of crystal growth [32,33]. We also observe that with increasing temperature CaHAP peaks slightly shift whereas KCl peaks slowly decrease before completely disappearing above 700 °C. Ionic chromatography analysis of the samples heated over 850 °C shows that chloride and potassium are still present, even if there are no longer visible on the XRD pattern. Comparison to JCPDS files indicates that tricalcium phosphate (β -TCP) is still present whereas chlorapatite seems to replace CaHAP. These results suggest that solid-state substitution reactions occur as already observed for calcium apatite [31]. They also underline that thermal treatment could be an efficient tool to control or to modify the structure of ashes and their components. As we observed [28] that washed ashes heated to 850 °C only present β -TCP and HAP. Further investigations would be necessary to get a full interpretation of the complex solid-state reaction.

4. Conclusion

The results show that meat and bone meal combustion residues are calcium (30.7%) and phosphate (56.3%) rich compounds, mainly a mixture of $\text{Ca}_{10}(\text{PO}_4)_6(\text{OH})_2$ and $\beta\text{-Ca}_3(\text{PO}_4)_2$. Significant levels of sodium (2.7%), potassium (2.5%) and magnesium (0.8%) are also observed. Ash particles are relatively small, from a few millimetre to micrometre, with almost 90% smaller than 1 mm.

Thermal conditions of MBM combustion (between 550 and 1000 °C) induce a wide range of structural modifications (crystallisation of calcium phosphate, substitution reaction, etc.), a strong decrease of the particles surface area (from 18 to 2 m²/g for ashes smaller than 250 μm), with a chemical composition remaining almost unchanged as shown by TGA analysis.

This work underlines the possibility to use this natural material as a low cost pure phosphate source with no heavy metal content (Ni, Cr or Cd), contrary to most natural phosphate ores. Identification of the major phases $\text{Ca}_{10}(\text{PO}_4)_6(\text{OH})_2$, $\beta\text{-Ca}_3(\text{PO}_4)_2$, NaCl, KCl allows us to better understand the chemical reactivity of ashes and to propose and investigate new valorisation processes such as phosphoric acid production, phosphate source for industry, agricultural soil enrichment, heavy metals immobilisation in soil or water, etc. as developed for phosphate rich compounds such as bones or rocks. Additional studies should be carried out to better understand how MBM combustion temperature modifies ashes structure and so ashes reactivity. Further progress in these areas should contribute value added outlets and help alleviate environmental concerns in a sustained development perspective.

Acknowledgements

The authors wish to thank Fersobio SA for providing meat and bone meal used in this work. We would also like to

thank the Chemistry Department of “IUT Paul Sabatier” for financial support and for offering accesses to some analytical equipment, L. Orts and T. Scandella for laboratory assistance.

References

- [1] D. Dormont, Prions, BSE and food, *Int. J. Food Microbiol.* 78 (2002) 181–189.
- [2] D. Taylor, Inactivation of the BSE agent, *C.R. Biol.* 325 (2002) 75–76.
- [3] D. Riesner, Prions and their biophysical background, *Biophys. Chem.* 66 (1997) 259–268.
- [4] P. Brown, P.P. Libersky, A. Wolf, D.C. Gajdusek, Resistance of scrapie infectivity to steam autoclaving after formaldehyde fixation and limited survival after ashing at 360 °C: practical and theoretical implications, *J. Infect. Dis.* 161 (1990) 467–472.
- [5] Rapport sur les risques sanitaires liés aux différents usages des farines et des graisses d'origine animale et aux conditions de leur traitement et de leur élimination, Avis de l'Agence Française de Sécurité Sanitaire des Aliments, 7 avril, 2001.
- [6] Syndicat des industries françaises de co-produits animaux (animals by-products french industries syndicate), <http://www.sifco.fr>.
- [7] Institut National de Recherche Agronomique (National Institute of Agronomic Research), <http://www.inra.fr>.
- [8] A. Chaala, C. Roy, Recycling of meat and bone meal animal feed by vacuum pyrolysis, *Environ. Sci. Technol.* 37 (2003) 4517–4522.
- [9] K.C. McDonnell, J. Desmond, J.J. Leahy, R. Howard-Hillidge, S. Ward, Behaviour of meat and bone meal/peat pellets in a bench scale fluidised bed combustor, *Energy* 26 (2001) 81–90.
- [10] J.A. Conesa, A. Fullana, R. Font, Thermal decomposition of meat and bone meal, *J. Anal. Appl. Pyrolysis* 70 (2003) 619–630.
- [11] H. Sis, S. Chander, Reagents used in the flotation of phosphate ores: a critical review, *Miner. Eng.* 16 (2003) 577–585.
- [12] Q.Y. Ma, T.J. Logan, S.J. Traina, Lead immobilisation from aqueous solutions and contaminated soils using phosphate rocks, *Environ. Sci. Technol.* 29 (1995) 1118–1126.
- [13] T. Suzuki, T. Hatsushika, Y. Hayakawa, Synthetic hydroxyapatite employed as inorganic cation-exchanger, *J. Chem. Soc., Faraday Trans.* 77 (1981) 1059–1062.
- [14] Y. Takeuchi, H. Arai, Removal of coexisting Pb^{2+} , Cu^{2+} and Cd^{2+} ions from water by addition of hydroxyapatite powder, *J. Chem. Eng. Jpn.* 23 (1990) 75–80.
- [15] Q.Y. Ma, T.J. Logan, S.J. Traina, Effects of NO_3^- , Cl^- , F^- , SO_4^{2-} and CO_3^{2-} on Pb^{2+} immobilisation by hydroxyapatite, *Environ. Sci. Technol.* 28 (1994) 408–418.
- [16] Q.Y. Ma, S.J. Traina, T.J. Logan, J.A. Ryan, Effects of aqueous Al, Cd, Cu, Fe(II), Ni and Zn on Pb immobilisation by hydroxyapatite, *Environ. Sci. Technol.* 28 (1994) 1219–1228.
- [17] Q.Y. Ma, S.J. Traina, T.J. Logan, J.A. Ryan, In situ lead immobilisation by apatite, *Environ. Sci. Technol.* 27 (1993) 1803–1810.
- [18] M.V. Ruby, A. Davis, A. Nicholson, In situ formation of lead phosphates in soils as a method to immobilise lead, *Environ. Sci. Technol.* 28 (1994) 646–654.
- [19] Y. Xu, F.W. Schwartz, S.J. Traina, Sorption of Zn^{2+} and Cd^{2+} on hydroxyapatite surfaces, *Environ. Sci. Technol.* 28 (1994) 1472–1480.
- [20] A.G. Leyva, J. Marrero, P. Smichowski, D. Cicerone, Sorption of antimony onto hydroxyapatite, *Environ. Sci. Technol.* 35 (2001) 3669–3675.
- [21] N.C.C. Da Rocha, R.C. De Campos, A.M. Rossi, E.L. Moreira, A.Do.F. Barbosa, G.T. Moure, Cadmium uptake by hydroxyapatite synthesised in different conditions and submitted to thermal treatment, *Environ. Sci. Technol.* 36 (2002) 1630–1635.
- [22] W. Admassu, T. Breeze, Feasibility of using natural fishbone apatite as a substitute for hydroxyapatite in remediating aqueous heavy metals, *J. Hazard. Mater. B* 69 (1999) 187–196.

- [23] F. Banat, S. Al-Asheh, F. Mohai, Batch zinc removal from aqueous solution using dried animal bones, *Separ. Purif. Technol.* 21 (2000) 155–164.
- [24] C.W. Cheung, J.F. Porter, G. McKay, Sorption kinetic analysis for the removal of cadmium ions from effluents using bone char, *Water Res.* 35 (2001) 605–612.
- [25] C.W. Cheung, J.F. Porter, G. McKay, Removal of Cu(II) and Zn(II) ions by sorption onto bone char using batch agitation, *Langmuir* 18 (2002) 650–656.
- [26] M.E. Hodson, E. Valsami-Jones, J.D. Cotter-Howells, Bone meal additions as a remediation treatment for metal contaminated soil, *Environ. Sci. Technol.* 34 (2000) 3501–3507.
- [27] E. Valsami-Jones, K.V. Ragnarsdottir, A. Putnis, D. Bosbach, A.J. Kemp, G. Cressey, The dissolution of apatite in the presence of aqueous metal cations at pH 2–7, *Chem. Geol.* 151 (1998) 215–233.
- [28] E. Deydier, R. Guilet, P. Scharrock, Beneficial use of meat and bone meal combustion residue: an efficient low cost material to remove lead from aqueous effluent, *J. Hazard. Mater. B* 101 (2003) 55–64.
- [29] M. Chen, L.Q. Ma, S.P. Singh, R.X. Cao, R. Melamed, Field demonstration of in situ immobilisation of soil Pb using P amendments, *Adv. Environ. Res.* 8 (2003) 93–102.
- [30] S. Raicevic, T. Kaludjerovic-Radoicic, A.I. Zouboulis, In situ stabilisation of toxic metals using phosphates: theoretical prediction and experimental verification, *J. Hazard. Mater. B* 117 (2005) 41–53.
- [31] J.C. Elliot, *Structure and Chemistry of the Apatites and Other Calcium Orthophosphates*, Elsevier, Netherlands, 1994, ISBN 0-444-81582-1.
- [32] J.L. Holden, P.P. Phakey, J.G. Clement, Scanning electron microscope observation of heat-treated human bone, *Foren. Sci. Int.* 74 (1995) 29–45.
- [33] M. Ozawa, S. Suzuki, Microstructural development of natural hydroxyapatite originated from fish-bone waste through heat treatment, *J. Am. Ceram. Soc.* 85 (2002) 1315–1317.